Color Image Registration Under Illumination Changes *

Raúl Montoliu[1], Pedro Latorre Carmona[2], and Filiberto Pla[2]

[1] Dept. Arquitectura y Ciéncias de los Computadores.
[2] Dept. Lenguajes y Sistemas Informáticos.
Jaume I University
Campus Riu Sec s/n 12071 Castellón, Spain
[montoliu,latorre,pla]@uji.es, http://www.vision.uji.es

Abstract. The estimation of parametric global motion has had a significant attention during the last two decades, but despite the great efforts invested, there are still open issues. One of the most important ones is related to the ability to recover large deformation between images in the presence of illumination changes while kipping accurate estimates. Illumination changes in color images are another important open issue. In this paper, a Generalized least squared-based motion estimator is used in combination with color image model to allow accurate estimates of global motion between two color images under the presence of large geometric transformation and illumination changes. Experiments using challenging images have been performed showing that the presented technique is feasible and provides accurate estimates of the motion and illumination parameters.

1 Introduction

Image registration ([17]) could be defined as the process to transform an image so that it matches another image as correctly as possible. This process is necessary when we want to compare or to integrate the data information from the two images. In the image acquisition process of a scene there are many factors involved: the position and the distance from the camera (or sensor) to the scene, the illumination, the nature of the objects to be imaged, etc. Any change in these factors implies that the data in the corresponding images are not directly comparable.

During the last few years, a special interest has emerged in relation to the need to cope with simultaneous viewpoint and illumination changes ([10], [12], [1], [2], to cite a few works). Important examples are those related to the retrieval of images in image databases where any user can upload an image of a famous place, and where each person may use different types of cameras and acquire the scene from different configurations and under different illumination conditions (cloudy, sunny, etc.).

There are evidently different methodologies to assess the best transformation between two images. One of them considers different versions of optimization-based motion estimation methods. Their main advantage is that the motion parameter estimation process is deeply over-constrained. Nevertheless, these methods suffer from a series of drawbacks [11]. One of the most important drawbacks is the presence of outliers, in the form of occlusions due to motion, to sensor noise, or to illumination changes.

* This work has been partially funded with project X from the Y.

In general, we may consider the *direct geometric registration problem* as that of minimizing an error function in relation to the difference in the pixel values between an image we may call *Test image* and the *Reference image*. In particular, it can be formally written as:

$$\min_{g} \sum_{\mathbf{q}\in\Re} \|\mathcal{I}_1(\mathbf{q_i}) - \mathcal{I}_2(\mathcal{G}(\mathbf{q_i};\mathbf{g}))\|^2 \tag{1}$$

where $\mathcal{I}_1$ and $\mathcal{I}_2$ are two input images, $\mathbf{q_i} = (x_i, y_i)^T$ are the pixel coordinates, $\mathbf{g}$ is the vector of motion parameters and $\mathcal{G}$ is the function to transform the pixel coordinates from one image to the other. The function $\mathcal{G}$ is expressed, for instance, in an affine (Eq. 2) motion (Eq. **??**) as follows:

$$\mathcal{G}(\mathbf{q_i};\mathbf{g}) = \begin{pmatrix} a_1 x_i + b_1 y_i + c_1 \\ a_2 x_i + b_2 y_i + c_2 \end{pmatrix} \tag{2}$$

If we also consider photometric changes, these may be modeled by a transformation $\mathcal{P}$ with parameter vector $\mathbf{p}$ and the minimization would therefore be:

$$\min_{g} \sum_{\mathbf{q}\in\Re} \|\mathcal{I}_1(\mathbf{q_i}) - \mathcal{P}(\mathcal{I}_2(\mathcal{G}(\mathbf{q_i};\mathbf{g})); \mathbf{p})\|^2 \tag{3}$$

To solve the problem shown in Eq. 3, Bartoli developed the *Dual Inverse Compositional* (DIC) estimation technique [2] where he considers Eq. 3 and then applies an inverse compositional update rule for both the geometric and photometric transformations. See [2] for details on the steps of the algorithm used to assess the geometric registration and illumination compensation parameters.

In this paper a generalized least squares-based non-linear motion estimation technique that incorporates the capability to deal with color illumination changes is presented, where illumination changes are modeled considering an affine transformation framework. The method is based on the GLS motion estimation method introduced by Montoliu and Pla in [11], and where a new set of functionals is proposed, incorporating these illumination changes. GLS method is applied on the functionals, deriving a new set of equations that allow the simultaneous assessment of the geometric and affine illumination transformation parameters. We show that the method we propose gives better results than the method recently described in [2].

The rest of the paper is organized as follows: section 2 justify bla bla. In Section **??** the GLS for general problems is briefly introduced. Section 4 presents our proposed method. Section 5 shows the experiments and results and finally we conclude in Section 6.

2 Illumination compensation model

Illumination compensation is closely related to what it is called *chromatic adaptation* in human colour vision. The first chromatic adaptation experiments started in the late 40s of the last century. A few years later, in a experiment made by Wyszecki and Stiles on *human asymmetric matching* [15], a human subject had different *adaptation states* on

two different parts of his visual field. The subject viewed a test light in one adaptation state and adjusted a mixture of three primary lights in the other adaptation state until the test light matched the mixture. They proved that a diagonal linear matrix transform would be enough to reproduce the experiment of asymmetric matching. Nevertheless, West and Brill [14] and others proved later that for a given set of sensor sensitivities a diagonal transform could only cover a restricted group of object colours and illuminant spectra.

Finlayson et al [3] reasoned that a diagonal transform would be enough for the modeling of an illumination change if the we may have extremely narrow-band sensors in the camera, which is often not the case. There are other cases where illumination compensation can fail, for instance, if there are other processes happening like bias in the camera, or saturated colours in the scene. In the latter case, some colours would *fall* in (and outside of) the camera gamut boundary [4]. This is the reason why the use of a complete (full) affine transform in the form $\mathbf{\Omega} \cdot \mathcal{I}(\mathbf{q}) + \mathbf{\Phi}$ is justified (see, for example, [5], [8], [16], to cite a few), where $\mathbf{\Omega} \in \Re^{3\times 3}$ is a full matrix, with elements ω_{kl}, $k, l = 1, \ldots, 3$, and $\mathbf{\Phi} \in \Re^3$, a vector with elements ϕ_k, $k = 1, \ldots, 3$.

3 GLS for general problems

In general, the GLS estimation problem can be expressed as follows (see [11] for more details):

$$\text{minimize } [\Theta_\upsilon = \upsilon^T \upsilon] \text{ subject to } \mathcal{F}(\chi, \lambda) = 0, \tag{4}$$

where:

- υ is a vector of r unknown residuals in the observation space, that is, $\upsilon = \lambda - \tilde{\lambda}$, where λ and $\tilde{\lambda}$ are the unperturbed and actually measured vector of observations, respectively.
- $\chi = (\chi^1, \ldots, \chi^m)^T$ is a vector of m parameters;
- λ is made up by r elements λ_i, $\lambda = (\lambda_1, \ldots, \lambda_r)^T$, each one is an observation vector with n components $\lambda_i = (\lambda_i^1, \ldots, \lambda_i^n)^T$
- $\mathcal{F}(\chi, \lambda)$ is made up by r elements $\mathcal{F}_i(\chi, \lambda_i)$, $\mathcal{F}(\chi, \lambda) = (\mathcal{F}_1(\chi, \lambda_1), \ldots, \mathcal{F}_r(\chi, \lambda_r))^T$, each one is, in general, a set of f functions that depend on the common vector of parameters χ and on an observation vector λ_i, $\mathcal{F}_i(\chi, \lambda_i) = (\mathcal{F}_i^1(\chi, \lambda_i), \ldots, \mathcal{F}_i^f(\chi, \lambda_i))^T$. Those functions can be non-linear.

Thus, the solution of (4) can be addressed as an iterative optimization starting with an initial guess of the parameters $\widehat{\chi}(0)$. At each iteration j, the algorithm estimates $\widehat{\Delta\chi}(j)$ to update the parameters as follows: $\widehat{\chi}(j) = \widehat{\chi}(j-1) + \widehat{\Delta\chi}(j)$. The process is stopped if the improvement $\widehat{\Delta\chi}(j)$ at iteration j is smaller than an user-specified resolution in the parameter space.

The improvement $\widehat{\Delta\chi}(j)$ can be expressed as follows (see [11] for more details):

$$\widehat{\Delta\chi}(j) = (\mathbf{A}^T\mathbf{Q}\mathbf{A})^{-1}\mathbf{A}^T\mathbf{Q}\mathbf{e}, \tag{5}$$

where the matrix $\mathbf{Q} = (\mathbf{B}\mathbf{B}^T)^{-1}$ has been introduced to simplify the notation. Equation 5 can also be expressed in a more convenient way as follows:

$$\widehat{\Delta\chi}(j) = \left(\sum_{i=1\ldots r} \mathbf{N}_i \right)^{-1} \left(\sum_{i=1\ldots r} \mathbf{T}_i, \right), \tag{6}$$

where $\mathbf{N}_i = \mathbf{A}_i^t(\mathbf{B}_i\mathbf{B}_i^t)^{-1}\mathbf{A}_i$ and $\mathbf{T}_i = \mathbf{A}_i^t(\mathbf{B}_i\mathbf{B}_i^t)^{-1}\mathbf{e}_i$, with

$$\mathbf{B}_i = \begin{pmatrix} \frac{\partial \mathcal{F}_i^1(\widehat{\chi}(j-1),\lambda_i)}{\partial \lambda_i^1} & \cdots & \frac{\partial \mathcal{F}_i^1(\widehat{\chi}(j-1),\lambda_i)}{\partial \lambda_i^n} \\ \vdots & & \vdots \\ \frac{\partial \mathcal{F}_i^f(\widehat{\chi}(j-1),\lambda_i)}{\partial \lambda_i^1} & \cdots & \frac{\partial \mathcal{F}_i^f(\widehat{\chi}(j-1),\lambda_i)}{\partial \lambda_i^n} \end{pmatrix}_{(f\times n)}, \tag{7}$$

$$\mathbf{A}_i = \begin{pmatrix} \frac{\partial \mathcal{F}_i^1(\widehat{\chi}(j-1),\lambda_i)}{\partial \chi^1} & \cdots & \frac{\partial \mathcal{F}_i^1(\widehat{\chi}(j-1),\lambda_i)}{\partial \chi^p} \\ \vdots & & \vdots \\ \frac{\partial \mathcal{F}_i^f(\widehat{\chi}(j-1),\lambda_i)}{\partial \chi^1} & \cdots & \frac{\partial \mathcal{F}_i^f(\widehat{\chi}(j-1),\lambda_i)}{\partial \chi^p} \end{pmatrix}_{(f\times m)}, \tag{8}$$

$$\mathbf{e}_i = \begin{pmatrix} -\mathcal{F}_i^1(\widehat{\chi}(j-1),\lambda_i) \\ \vdots \\ -\mathcal{F}_i^f(\widehat{\chi}(j-1),\lambda_i) \end{pmatrix}_{(f\times 1)}. \tag{9}$$

4 GLS-based color motion estimation under illumination changes

In our formulation of the motion estimation problem, the function $\mathcal{F}_i(\chi,\lambda_i)$ is expressed as follows:

$$\mathcal{F}_i(\chi,\lambda_i) = \mathcal{I}_2(\mathcal{G}(\mathbf{q}_i;\mathbf{g})) - \mathcal{P}^{-1}(\mathcal{I}_1(\mathbf{q}_i);\mathbf{p}) \tag{10}$$

$\mathcal{I}_1(\mathbf{q}_i) = (R_1(\mathbf{q}_i), G_1(\mathbf{q}_i), B_1(\mathbf{q}_i))^T$ and $\mathcal{I}_2(\mathbf{q}_i') = (R_2(\mathbf{q}_i'), G_2(\mathbf{q}_i'), B_2(\mathbf{q}_i'))^T$, where $\mathbf{q}_i'$ has been introduced to simplify notation as: $\mathbf{q}_i' = \mathcal{G}(\mathbf{q}_i;\mathbf{g})$. Note that in this case the number of functions f is 3. The Eq. 10 can also be writen in a more convient way as follows:

$$\begin{aligned} \mathcal{F}_i^1(\chi,\lambda_i) &= R_2(\mathbf{q}_i') - (R_1(\mathbf{q}_i)\omega_{11} + G_1(\mathbf{q}_i)\omega_{12} + B_1(\mathbf{q}_i)\omega_{13} + \phi_1) \\ \mathcal{F}_i^2(\chi,\lambda_i) &= G_2(\mathbf{q}_i') - (R_1(\mathbf{q}_i)\omega_{21} + G_1(\mathbf{q}_i)\omega_{22} + B_1(\mathbf{q}_i)\omega_{23} + \phi_2) \\ \mathcal{F}_i^3(\chi,\lambda_i) &= B_2(\mathbf{q}_i') - (R_1(\mathbf{q}_i)\omega_{31} + G_1(\mathbf{q}_i)\omega_{32} + B_1(\mathbf{q}_i)\omega_{33} + \phi_3) \end{aligned} \tag{11}$$

where $R_1(\mathbf{q}_i)$, $G_1(\mathbf{q}_i)$ and $B_1(\mathbf{q}_i)$ are the R, G and B, components of the first color image in the sequence (reference image) at the point $\mathbf{q}_i$, and $R_2(\mathbf{q}_i')$, $G_2(\mathbf{q}_i')$ and $B_2(\mathbf{q}_i')$ are the R, G and B, components of the second color image in the sequence (test image) at the transformed point $\mathbf{q}_i' = \mathcal{G}(\mathbf{q}_i;\mathbf{g})$. In this case, each observation vector λ_i is related to each pixel q_i, with r being the number of pixels in the area of interest.

Let us define the observation vector as $\lambda_i = (R_1(\mathbf{q}_i), G_1(\mathbf{q}_i), B_1(\mathbf{q}_i), x_i, y_i)$. The vector of parameters is defined as follows: $\chi = (\mathbf{g}, \mathbf{p})^T$.

Due to the big dimension of the parameter vector it is difficult to show $\mathbf{A}_i$, $\mathbf{B}_i$ using matrices. We use tables intead. For afine motion, The $\mathbf{A}_i$ matrix is showed in two tables: 1 and 2; $\mathbf{B}_i$ is showed in two tables: 3 and 4. For projective motion, The $\mathbf{A}_i$ matrix is showed in two tables: 5 and 2; $\mathbf{B}_i$ is showed in two tables: 3 and 6.

Function	∂a_1	∂b_1	∂c_1	∂a_2	∂b_2	∂c_2
$\mathcal{F}_1(\chi, \lambda_i)$	$x_i R_2^x$	$y_i R_2^x$	R_2^x	$x_i R_2^y$	$y_i R_2^y$	R_2^y
$\mathcal{F}_2(\chi, \lambda_i)$	$x_i G_2^x$	$y_i G_2^x$	G_2^x	$x_i G_2^y$	$y_i G_2^y$	G_2^y
$\mathcal{F}_3(\chi, \lambda_i)$	$x_i B_2^x$	$y_i B_2^x$	B_2^x	$x_i B_2^y$	$y_i B_2^y$	B_2^y

Table 1. $\mathbf{A}_i$ matrix for affine motion. First part.

Function	$\partial\alpha_{11}$	$\partial\alpha_{12}$	$\partial\alpha_{13}$	$\partial\alpha_{21}$	$\partial\alpha_{22}$	$\partial\alpha_{23}$	$\partial\alpha_{31}$	$\partial\alpha_{32}$	$\partial\alpha_{33}$	$\partial\beta_1$	$\partial\beta_2$	$\partial\beta_3$
$\mathcal{F}_1(\chi, \lambda_i)$	$-R_1$	$-G_1$	$-B_1$	0	0	0	0	0	0	-1	0	0
$\mathcal{F}_2(\chi, \lambda_i)$	0	0	0	$-R_1$	$-G_1$	$-B_1$	0	0	0	0	-1	0
$\mathcal{F}_3(\chi, \lambda_i)$	0	0	0	0	0	0	$-R_1$	$-G_1$	$-B_1$	0	0	-1

Table 2. $\mathbf{A}_i$ matrix for affine and projective motion. Second part.

Function	∂R_1	∂G_1	∂B_1
$\mathcal{F}_1(\chi, \lambda_i)$	$-\alpha_{11}$	$-\alpha_{12}$	$-\alpha_{13}$
$\mathcal{F}_2(\chi, \lambda_i)$	$-\alpha_{21}$	$-\alpha_{22}$	$-\alpha_{23}$
$\mathcal{F}_3(\chi, \lambda_i)$	$-\alpha_{31}$	$-\alpha_{32}$	$-\alpha_{33}$

Table 3. $\mathbf{B}_i$ matrix for affine and projective motion. First part

In the Tables, R_1^x, R_1^y, R_2^x, R_2^y, G_1^x, G_1^y, G_2^x, G_2^y, B_1^x, B_1^y, B_2^x and B_2^y have been introduced to simplify notation as follows: $R_1^x(\mathbf{q}_i)$, $R_1^y(\mathbf{q}_i)$, $R_2^x(\mathbf{q}'_i)$, $R_2^y(\mathbf{q}'_i)$, $G_1^x(\mathbf{q}_i)$, $G_1^y(\mathbf{q}_i)$, $G_2^x(\mathbf{q}'_i)$, $G_2^y(\mathbf{q}'_i)$, $B_1^x(\mathbf{q}_i)$, $B_1^y(\mathbf{q}_i)$, $B_2^x(\mathbf{q}'_i)$ and $B_2^y(\mathbf{q}'_i)$, respectively, being $R_1^x(\mathbf{q}_i)$, $R_1^y(\mathbf{q}_i)$,$G_1^x(\mathbf{q}_i)$, $G_1^y(\mathbf{q}_i)$, $B_1^x(\mathbf{q}_i)$, $B_1^y(\mathbf{q}_i)$, the components of the gradient of the R, G, B bands, respectively, of test image at point $\mathbf{q}_i$; and $R_2^x(\mathbf{q}'_i)$, $R_2^y(\mathbf{q}'_i)$, $G_2^x(\mathbf{q}'_i)$, $G_2^y(\mathbf{q}'_i)$, $B_2^x(\mathbf{q}'_i)$, $B_2^y(\mathbf{q}'_i)$ the components of the gradient of the R,G,B bands, respectively, of the reference image at point $\mathbf{q}'_i$.

In addition, N_d, N_1, N_2, N_3, N_4, N_5 and N_6 have also been introduced as follows:

Function	∂x	∂y
$\mathcal{F}_1(\chi,\lambda_i)$	$(a_1R_2^x + a_2R_2^y) - (\alpha_{11}R_1^x + \alpha_{12}G_1^x + \alpha_{13}B_1^x)$	$(b_1R_2^x + b_2R_2^y) - (\alpha_{11}R_1^y + \alpha_{12}G_1^y + \alpha_{13}B_1^y)$
$\mathcal{F}_2(\chi,\lambda_i)$	$(a_1G_2^x + a_2G_2^y) - (\alpha_{21}R_1^x + \alpha_{22}G_1^x + \alpha_{23}B_1^x)$	$(b_1G_2^x + b_2G_2^y) - (\alpha_{21}R_1^y + \alpha_{22}G_1^y + \alpha_{23}B_1^y)$
$\mathcal{F}_3(\chi,\lambda_i)$	$(a_1B_2^x + a_2B_2^y) - (\alpha_{31}R_1^x + \alpha_{32}G_1^x + \alpha_{33}B_1^x)$	$(b_1B_2^x + b_2B_2^y) - (\alpha_{31}R_1^y + \alpha_{32}G_1^y + \alpha_{33}B_1^y)$

Table 4. $\mathbf{B}_i$ matrix for affine motion. Second part

function	∂a_1	∂b_1	∂c_1	∂a_2	∂b_2	∂c_2	∂d	∂e
$\mathcal{F}_1(\chi,\lambda_i)$	$\frac{xR_2^x}{N_d}$	$\frac{yR_2^x}{N_d}$	$\frac{R_2^x}{N_d}$	$\frac{xR_2^y}{N_d}$	$\frac{yR_2^y}{N_d}$	$\frac{R_2^y}{N_d}$	$\frac{-x_iR_2^xN_1 - x_iR_2^yN_2}{N_d^2}$	$\frac{-y_iR_2^xN_1 - y_iR_2^yN_2}{N_d^2}$
$\mathcal{F}_2(\chi,\lambda_i)$	$\frac{xG_2^x}{N_d}$	$\frac{yG_2^x}{N_d}$	$\frac{G_2^x}{N_d}$	$\frac{G_2^y}{N_d}$	$\frac{yG_2^y}{N_d}$	$\frac{G_2^y}{N_d}$	$\frac{-x_iG_2^xN_1 - x_iG_2^yN_2}{N_d^2}$	$\frac{-y_iG_2^xN_1 - y_iG_2^yN_2}{N_d^2}$
$\mathcal{F}_3(\chi,\lambda_i)$	$\frac{xB_2^x}{N_d}$	$\frac{yB_2^x}{N_d}$	$\frac{B_2^x}{N_d}$	$\frac{xB_2^y}{N_d}$	$\frac{yB_2^y}{N_d}$	$\frac{B_2^y}{N_d}$	$\frac{-x_iB_2^xN_1 - x_iB_2^yN_2}{N_d^2}$	$\frac{-y_iB_2^xN_1 - y_iB_2^yN_2}{N_d^2}$

Table 5. $\mathbf{A}_i$ matrix for projective motion. First part.

$$
\begin{aligned}
&N_d = (dx_i + ey_i + 1)\\
&N_1 = a_1x_i + b_1y_i + c_1, N_2 = a_2x_i + b_2y_i + c_2\\
&N_3 = \frac{a_1N_d - dN_1}{N_d^2}, N_4 = \frac{a_2N_d - dN_2}{N_d^2}\\
&N_5 = \frac{b_1N_d - eN_1}{N_d^2}, N_6 = \frac{b_2N_d - eN_2}{N_d^2}
\end{aligned}
\tag{12}
$$

The estimation process is resumed at Algorithm 1. A Feature Step is used to initialize the motion estimator (whenever the deformation between images is quite large we need a good initial vector of motion parameters). It mainly consists of a SIFT-based technique [9] to detect and describe interest points, where for each interest point belonging to the first image a *K-NN* search strategy is performed to find the k-closest interest points at the second image. Finally, for estimating the first approximation of the motion parameters a random sampling technique is used [13].

Regarding the illumination parameters at $\widehat{\chi}(0)$, they have initially been set to: $\Omega = \mathbf{I}$ and $\Phi = (0,0,0)^T$.

5 Experiments and Results

In order to test the accuracy of the proposed motion estimation technique, several experiments have been perfomed using a set of challeging images. A preview of some

function	∂x	∂y
$\mathcal{F}_1\chi,\lambda_i$	$(N_3R_2^x + N_4R_2^y) - (\alpha_{11}R_1^x + \alpha_{12}G_1^x + \alpha_{13}B_1^x)$	$(N_5R_2^x + N_6R_2^y) - (\alpha_{11}R_1^y + \alpha_{12}G_1^y + \alpha_{13}B_1^y)$
$\mathcal{F}_2\chi,\lambda_i$	$(N_3G_2^x + N_4G_2^y) - (\alpha_{21}R_1^x + \alpha_{22}G_1^x + \alpha_{23}B_1^x)$	$(N_5G_2^x + N_6G_2^y) - (\alpha_{21}R_1^y + \alpha_{22}G_1^y + \alpha_{23}B_1^y)$
$\mathcal{F}_3\chi,\lambda_i$	$(N_3B_2^x + N_4B_2^y) - (\alpha_{31}R_1^x + \alpha_{32}G_1^x + \alpha_{33}B_1^x)$	$(N_5B_2^x + N_6B_2^y) - (\alpha_{31}R_1^y + \alpha_{32}G_1^y + \alpha_{33}B_1^y)$

Table 6. $\mathbf{B}_i$ matrix for proyective motion. Second part

Input: Images $I_1 = (R_1, G_1, B_1)^T$ and $I_2 = (R_2, G_2, B_2)^T$
Output: $\widehat{\chi}$, the vector of estimated motion parameters.
1: Calculate image gradients.
2: $j = 0$.
3: Set $\Omega_0 = \mathbf{I}$, $\Phi_0 = (0, 0, 0)^T$ and $\mathbf{g}_0 = \text{FeatureStep}(I_1, I_2)$.
4: $\widehat{\chi}(0) = (\mathbf{g}_0, \mathbf{p}_0)^T$, with $\mathbf{p}_0 = (\omega_{11}, \ldots, \omega_{33}, \phi_1, \ldots, \phi_3)$.
5: **repeat**
6: $j = j + 1$.
7: Update matrices $\mathbf{A}_i$, $\mathbf{B}_i$ and $\mathbf{e}_i$ using $\widehat{\chi}(j-1)$.
8: Estimate $\widehat{\Delta\chi}(j)$.
9: $\widehat{\chi}(j) = \widehat{\chi}(j-1) + \widehat{\Delta\chi}(j)$.
10: **until** $|\widehat{\Delta\chi}(j)|$ is small enough.
11: $\widehat{\chi} = \widehat{\chi}(j)$.

Algorithm 1: Generalized Least Squares motion estimation algorithm

of them is shown in Figure 1. In all image pairs there exists a geometric tranformation simultaneus to a photometric one. Theses images have been obtained from several sources, including: Bartoli's examples [3], Brainard's examples [4], Simon Fraser University Computational Vision Lab's examples [5] and Oxford's Visual Geometry Group's examples [6]. Finally, the last four have been acquired by ourselves using a conventional digital camera and varying the ilumination conditions.

The *Dual Inverse Compositional* technique [2] was used for comparison purposes since it is, as far as we known, the only other technique that estimates simultaneuosly the motion and the illumination parameters in color images. For each image pair, first, the feature step is performed to obtain a good inital motion parameters. Then, both algorithms are executed, obtaining two output parameters χ_{GLS} and χ_{DIC}. With the estimated parameters, the reference image can be transformed (geometrically and photometrically). Then if the parameters have been correctly estimated, the resulting images ($\mathcal{I}_{GLS}$ and $\mathcal{I}_{DIC}$) have to be very similar to the corresponding reference images. Figure 2 shows the results obtained with the proposed technique for Bartoli's images. First row shows the test and the reference image. Second row shows the resulting image and the panoramic image created. Note how both, the motion and the illumination parameters have been correctly estimated.

Once the resulting images ($\mathcal{I}_{GLS}$ and $\mathcal{I}_{DIC}$) have been created it is possible to apply a merit figure to measure to quality of the registration. Four similarity measures have been used. They are the Normalized Correlation Coefficient (NCC), the Increment Sign Correlation coefficient (ISC [6]), the selective correlation Coefficient (SCC [7]) and the Normalized Average of Absolute errors ($NAAE$) defined as:

[3] `http://www.lasmea.univ-bpclermont.fr/Personnel/Adrien.Bartoli/Research/DirectImageRegistration/index.html`
[4] `http://color.psych.upenn.edu/brainard/`
[5] `http://www.cs.sfu.ca/~colour/data/objects_under_different_lights/index.html`
[6] `http://www.robots.ox.ac.uk/~vgg/research/affine/index.html`

Fig. 1. Input images

$$NAAE(aae) = \begin{cases} 0 \text{ if } aae > TH \\ (TH - aae)/TH \text{ otherwise} \end{cases}, \tag{13}$$

where aae is the average of the absolute errors and TH is a constant.

The four measures produce values from 0 (low similarity) to 1 (high similarity). Figure 3 shows the average of the values obtained for all experiments. Note how the proposed estimation technique overcomes Bartoli's one for all similarity measures.

6 Conclusions

bla bla

References

1. A. Bartoli. Groupwise geometric and photometric direct image registration. In *Proceedings of the British Machine Vision Conference*, 2006.
2. A. Bartoli. Groupwise geometric and photometric direct image registration. *IEEE Transactions on Pattern Analysis and Machine Intelligence*, 30:2098–2108, 2008.
3. G. D. Finlayson, Mark S. Drew, and Brian V. Funt. Color constancy: generalized diagonal transforms suffice. *Journal of the Optical Society of America, A*, 11:3011–3019, 1994.
4. G. D. Finlayson, S. D. Hordley, and R. Xu. Convex programming colour constancy with a diagonal-offset model. In *IEEE ICIP*, 2005.
5. G. Healey and A. Jain. Retrieving multispectral satellite images using physics-based invariant representations. *IEEE Transactions on Pattern Analysis and Machine Intelligence*, 18:842–848, 1996.
6. Shunichi Kaneko, Ichiro Murase, and Satoru Igarashi. Robust image registration by increment sign correlation. *Pattern Recognition*, 35(10):2223–2234, 2002.

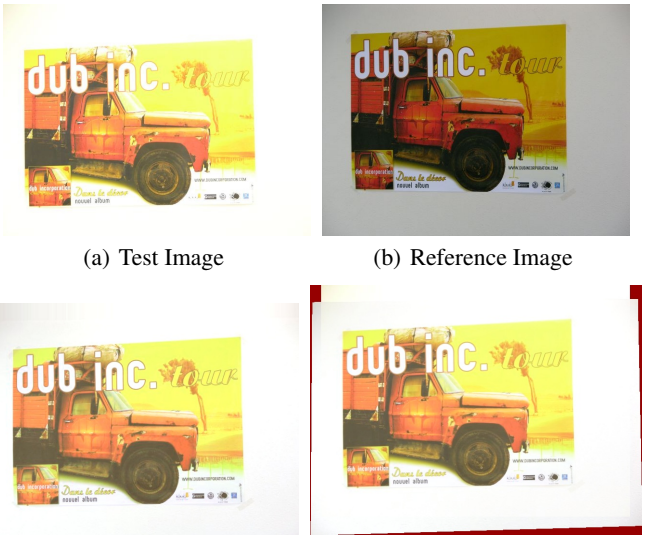

(a) Test Image (b) Reference Image

(c) Resulting image (d) Panoramic Image

Fig. 2. Results

7. Shunichi Kaneko, Yutaka Satoh, and Satoru Igarashi. Using selective correlation coefficient for robust image registration. *Pattern Recognition*, 36(5):1165–1173, 2003.
8. R. Lenz, L. V. Tran, and P. Meer. Moment based normalization of color images. In *IEEE 3rd Workshop on multimdeia signal processing*, pages 103–108, 1998.
9. D. G. Lowe. Distinctive image features from scale-invariant keypoints. *International Journal of Computer Vision*, 60(2):91–110, 2004.
10. F. Mindru, T. Tuytelaars, L. V. Gool, and T. Moons. Moment invariants for recognition under changing viewpoint and illumination. *Computer Vision and Image Understanding*, 94:3–27, 2004.
11. Raúl Montoliu and Filiberto Pla. Generalized least squares-based parametric motion estimation. *Computer Vision and Image Understanding*, 113(7):790–801, July 2009.
12. L. Shao and M. Brady. Invariant salient regions based image retrieval under viewpoint and illumination variations. *J. Vis. Commun. Image R.*, 17:1256–1271, 2006.
13. P. H. S. Torr and A. Zisserman. Mlesac: A new robust estimator with application to estimating image geometry. *Computer Vision and Image Understanding*, 78:138–156, 2000.
14. G. West and M. H. Brill. Necessary and sufficient conditions for von kries chromatic adaptation to give color constancy. *J. Math. Biol.*, 15:249–258, 1982.
15. G. Wyszecki and W.S. Stiles. *Color science*. John Wiley & Sons, 1967.
16. Z. Xingming and Z. Huangyuan. An illumination independent eye detection algorithm. In *IEEE ICPR*, 2006.
17. B. Zitova and J. Flusser. Image registration methods: a survey. *Image and Vision Computing*, 21:997–1000, 2003.

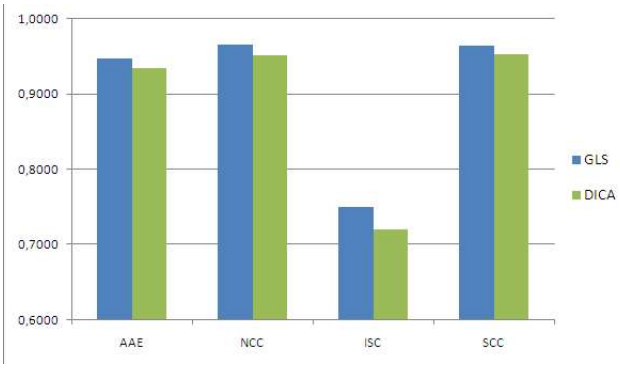

Fig. 3. Registration results